The Bending-Gradient theory for flexural wave propagation in composite plates

Nadine Bejjani, Pierre Margerit, Karam Sab, Joanna Bodgi, Arthur Lebée

▶ To cite this version:

The Bending-Gradient theory for wave propagation in composite plates

Nadine Bejjani[1-2], Pierre Margerit[1], Karam Sab[1*], Joanna Bodgi[2], Arthur Lebée[1]

[1]*Laboratoire Navier, UMR 8205, École des Ponts ParisTech, IFSTTAR, CNRS, Université Paris Est 6-8 av. Blaise Pascal, Cité Descartes, 77420 Champs sur Marne, France*

[2]*Unité de recherche « Mathématiques et modélisation », Faculté des sciences, Université Saint-Joseph, B.P. 11-514 Riad El Solh Beyrouth 1107 2050, Lebanon.*

Abstract

This paper is concerned with the prediction of the propagation of flexural waves in anisotropic laminated plates with relatively high slenderness ratios by means of refined plate models. The study is conducted using the Bending-Gradient theory which is considered as an extension of the Reissner-Mindlin theory to multilayered plates. Two projections of the Bending-Gradient model on Reissner-Mindlin models are also explored. The relevance of the proposed models is tested by comparing them to well-known plate theories and to reference results obtained using the finite element method.

Keywords: Wave propagation, Dispersion curve, Flexural mode, Laminated plates, Three-dimensional elasticity, Bending-Gradient theory, Reissner-Mindlin model, Spectral Finite Element Method

1. Introduction

Owing to their lightweight and advanced high strength, composite plates are widely used in the civil, marine, aerospace and automotive industries. Due to their anisotropic and heterogeneous nature, the accurate prediction of their structural behavior is a challenging problem that has stimulated considerable research interest. Several plate theories have been proposed in the literature. The most well-known and simplest are the Kirchhoff-Love theory (or Classical Plate Theory) for thin plates (Kirchhoff, 1850a,b, Love, 1888) and the Reissner-Mindlin theory (or First Order Shear Deformation Theory) for thin to moderately thick

plates (Reissner, 1945, Mindlin, 1951). The Kirchhoff-Love and the Reissner-Mindlin models provide very satisfactory results when the constitutive material is homogeneous (Ciarlet and Destuynder, 1979, G. Ciarlet, 1990, 1997). However, the extension of these models to heterogeneous plates leads to discontinuous out of plane shear distributions and incorrect estimation of the deflection compared to exact solutions (Yang et al., 1966, M. Whitney and J. Pagano, 1970). Limitations of the Kirchhoff-Love and Reissner-Mindlin models induced the development of higher order models in order to capturing correctly the effects of out of plane shear deformations (M. Whitney, 1972, Reddy, 1989, Noor and Malik, 2000, Carrera, 2002).

In the light of the ideas presented by Reissner, Lebée and Sab (2011) have recently derived a new model, known as the Bending-Gradient theory, dedicated to thick and anisotropic plates. Here, the classical Reissner-Mindlin out-of-plane shear forces are replaced by the generalized shear force related to the first gradient of the bending moment. Furthermore, six rotations are introduced instead of two. This is why the Bending-Gradient theory is considered as an extension of the Reissner-Mindlin theory to laminated plates. The reader is referred to Sab and Lebée (2015) for thorough details. It was demonstrated that the Bending-Gradient model cannot be reduced to a Reissner-Mindlin model unless the constitutive material of the plate is homogeneous (Lebée and Sab, 2011). For this reason, these authors searched for an approximation of the Bending-Gradient model by a suitable Reissner-Mindlin model (Lebée and Sab, 2015). Several projections of the Bending-Gradient model were discussed and their relevance was tested (Sab and Lebée, 2015). Comparisons with the Reissner-Mindlin theory and the full three-dimensional exact solutions (Pagano, 1969, 1970) showed that the Bending-Gradient theory gives good prediction of deflection, shear stress distributions and in-plane displacement distributions in any material configuration. Originally designed for laminated plates, the Bending-Gradient theory was extended to in-plane periodic plates, sandwich panels (Lebée and Sab, 2012a,b), space frames (Lebée and Sab, 2013) and applied to cross laminated timber panels (Perret et al., 2016).

In recent papers, the Bending-Gradient theory was justified through asymptotic expansions (Lebée and Sab, 2013) as well as variational methods and a series of existence and

uniqueness theorems were formulated and proved (Bejjani et al., 2018). Having mathematically justified this theory, the central aim of this work is to test its validity regarding plane wave propagation in symmetrical anisotropic heterogeneous plates. Since plane waves propagate in unbounded elastic continua, the plate is considered to be infinite in the direction of wave propagation, away from boundary conditions and loadings. While the classical plate theory agrees well with the analytical solutions when the wavelength λ is very large with respect to the thickness h, our results show that it becomes invalid when the thickness-wavelength (h/λ) ratio is greater than 0.05 approximately. In this paper, we go further in the approximation and focus on wavelengths that are about two times the laminate thickness $(h/\lambda = 0.5)$. It is expected that the Bending-Gradient theory will fail to give acceptable results beyond this limit. In fact, modelling a plate as a two-dimensional domain and ignoring the contributions in the transverse direction is not valid when the wavelength is about or less than the plate thickness. In what follows, we seek to relate the wave number and the angular frequency for the sake of predicting dispersion curves of flexural waves, i.e waves whose displacements are perpendicular to the direction of propagation.

Analytical solutions for the wave propagation problem in composite materials are difficult to determine. One of the most used methods to solve such problems is the Finite Element Analysis. Different methodologies have been developed over the years, the foremost being the Semi-Analytical Finite Element method (SAFE) Kausel (1986), Datta et al. (1988). Recently, Gravenkamp et al. (2012) presented a formulation of the wave propagation problem based on the Scaled Boundary Finite Element Method (SBFEM). Mention may also be made of Renno et al. (2013), who described the Wave Finite Element (WFE) approach which besides being simple in application, provides accurate results at low computational cost. In order to verify the relevance of the Bending-Gradient model and its projections on Reissner-Mindlin models, a comparative study between our results and those obtained by the finite element analysis of the three-dimensional problem detailed in Margerit (2018) is conducted.

The paper proceeds as follows. In Section 2, we introduce tensor notations and algebraic manipulations that are used throughout this paper. Section 3 concisely provides the

3

main definitions and equations of the Bending-Gradient model for anisotropic heterogeneous plates. The particular case of homogeneous plates is also discussed and projections of the Bending-Gradient theory on a Reissner-Mindlin plate theory are presented. Section 4 is concerned with the derivation and the implementation of the plane waves dispersion curves either in 3D or from a plate model. Finally, in Section 5, we verify the accuracy of the proposed method by comparing results from the classical plate theory (CPT), the first order shear deformation theory (FOSDT), the Bending-Gradient theory (BG) and the proposed projections (SSP and SCP) to results computed using the finite element method. Conclusions are given in Section 6.

2. Notations

In this paper, we use Greek indices for 2D tensors (α, β, $\gamma.. = 1, 2$) and Latin indices for 3D tensors (i, j, $k.. = 1, 2, 3$). For example, ($X_{\alpha\beta}$) represents the 2D tensor while (X_{ij}) denotes a 3D tensor . Index notation also provides another advantage: the number of indices indicates the order of the tensor. For example, (X_{ij}) denotes a second-rank tensor whereas (X_{ijkl}) denotes a fourth-rank tensor. To simplify expressions including tensors, we shall make use of the Einstein summation convention according to which all indices appearing twice within an expression are to be summed.

The identity for 2D vectors is ($\delta_{\alpha\beta}$) where $\delta_{\alpha\beta}$ is Kronecker symbol ($\delta_{\alpha\beta} = 1$ if $\alpha = \beta$, $\delta_{\alpha\beta} = 0$ otherwise). The identity for 2D symmetric second order tensors is $i_{\alpha\beta\gamma\delta}$ where $i_{\alpha\beta\gamma\delta} = \frac{1}{2}\left(\delta_{\alpha\gamma}\delta_{\beta\delta} + \delta_{\alpha\delta}\delta_{\beta\gamma}\right)$. The reader might easily check that $i_{\alpha\beta\gamma\delta}i_{\delta\gamma\eta\theta} = i_{\alpha\beta\eta\theta}$, $i_{\alpha\beta\gamma\delta}i_{\delta\gamma\beta\theta} = 3/2\delta_{\alpha\theta}$ and $i_{\alpha\beta\gamma\delta}i_{\delta\gamma\beta\alpha} = 3$.

The gradient of a scalar field X writes ($X_{,\beta}$) while the gradient of a vector or a higher-order tensor fields writes ($X_{\alpha\beta,\gamma}$), for instance. The divergence of a vector field or a second order tensor field is noted ($X_{\alpha,\alpha}$) and ($X_{\alpha\beta,\beta}$), respectively.

Finally, the integration through the thickness is noted $\langle\bullet\rangle$: $\int_{-\frac{h}{2}}^{\frac{h}{2}} f(x_3)dx_3 = \langle f\rangle$.

3. The Bending-Gradient Model for the equilibrium of thick plates

3.1. The 3D plate configuration

The physical space is endowed with an orthonormal reference frame $(O, \underline{e}_1, \underline{e}_2, \underline{e}_3)$ where O is the origin and $\underline{e}_i$ is the base vector in direction $i \in \{1, 2, 3\}$. We consider a linear elastic plate occupying the 3D domain $V = S \times \left] -\frac{h}{2}, \frac{h}{2} \right[$, where $S \subset \mathbb{R}^2$ is the middle surface of the plate and h its thickness. The boundary of the domain, denoted by ∂V, is decomposed intro three parts (Figure 1):

$$\partial V = \partial V_{\text{lat}} \cup \partial V_3^+ \cup \partial V_3^-,$$

$$\text{with} \quad \partial V_{\text{lat}} = \partial S \times \left] -\frac{h}{2}, \frac{h}{2} \right[\quad \text{and} \quad \partial V_3^\pm = S \times \left\{ \pm \frac{h}{2} \right\}, \tag{1}$$

where ∂S is the boundary of S.

Focusing only on out-of-plane loadings, the plate is subjected to forces per unit surface on $\partial V_3^\pm$ of the form:

$$(T_1, T_2, T_3)^\pm (x_1, x_2) = \left(0, 0, \frac{1}{2} p(x_1, x_2) \right), \tag{2}$$

where p is a given function on S.

We suppose that the constitutive material is invariant with respect to translations in
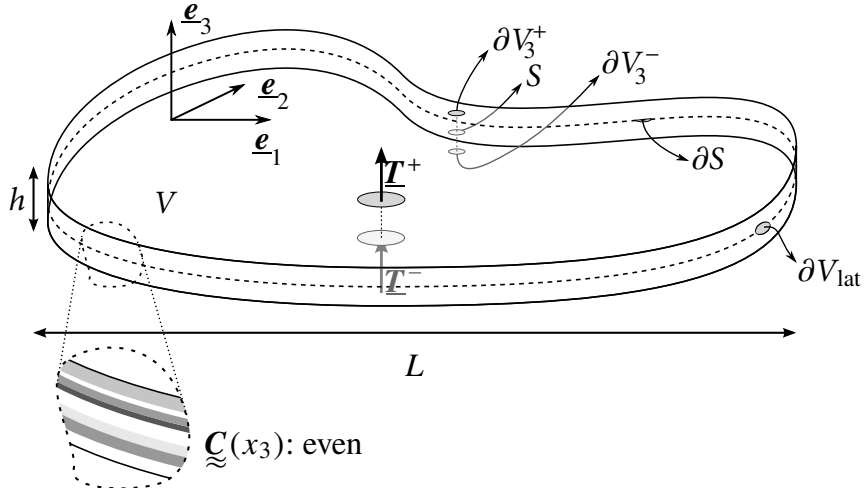

Figure 1: The 3D configuration

the (x_1, x_2) plane. Therefore, the fourth-rank 3D elasticity stiffness tensor (C_{ijkl}) does not depend on (x_1, x_2). The plate is assumed to be symmetric with respect to its mid-plane S, hence C_{ijkl} is an even function of x_3:

$$C_{ijkl}(x_3) = C_{ijkl}(-x_3). \tag{3}$$

This is the so-called mirror symmetry. Furthermore, we have that:

$$C_{3\alpha\beta\gamma} = C_{\alpha333} = 0. \tag{4}$$

In this case, the constitutive material is said to be monoclinic.

To make the presentation self-contained, we now briefly recall the main definitions of the kinematic and static fields of the Bending-Gradient theory as well as the governing equations established by Lebée and Sab (2011). For more details concerning the Bending-Gradient theory, the reader is referred to Lebée and Sab (2011), Lebée and Sab (2011), Lebée and Sab (2015), Lebée and Sab (2015), Sab and Lebée (2015) and Bejjani et al. (2018).

3.2. The Bending-Gradient equations

The Bending-Gradient generalized displacements are $(U_3, \Phi_{\alpha\beta\gamma})$ where U_3 is the out-of-plane displacement of the plate (or deflection) and $(\Phi_{\alpha\beta\gamma})$ is the generalized rotation tensor with $\Phi_{\alpha\beta\gamma} = \Phi_{\beta\alpha\gamma}$.

The Bending-Gradient generalized strains, which derive from $(U_3, \Phi_{\alpha\beta\gamma})$ are $(\chi_{\alpha\beta}, \Gamma_{\alpha\beta\gamma})$. $(\chi_{\alpha\beta})$ is the curvature second-order tensor with $\chi_{\alpha\beta} = \chi_{\beta\alpha}$, and $(\Gamma_{\alpha\beta\gamma})$ is the generalized shear strain verifying $\Gamma_{\alpha\beta\gamma} = \Gamma_{\beta\alpha\gamma}$. The generalized strains are obtained through the following compatibility conditions on S:

$$\begin{cases} \chi_{\alpha\beta} = \Phi_{\alpha\beta\gamma,\gamma}, & \text{(5a)} \\ \Gamma_{\alpha\beta\gamma} = \Phi_{\alpha\beta\gamma} + i_{\alpha\beta\gamma\delta} U_{3,\delta}. & \text{(5b)} \end{cases}$$

The Bending-Gradient generalized strains $(\chi_{\alpha\beta}, \Gamma_{\alpha\beta\gamma})$ constitute the dual of the Bending-Gradient generalized stresses $(M_{\alpha\beta}, R_{\alpha\beta\gamma})$. The second-order tensor $(M_{\alpha\beta})$ is the conventional bending moment tensor $(M_{\alpha\beta} = M_{\beta\alpha})$ related to the 3D local stress (σ_{ij}) by:

$$M_{\alpha\beta} = \langle x_3 \sigma_{\alpha\beta} \rangle. \tag{6}$$

6

The third-order tensor $(R_{\alpha\beta\gamma})$ represents the generalized shear force which complies with the following symmetry: $R_{\alpha\beta\gamma} = R_{\beta\alpha\gamma}$. The Bending-Gradient constitutive equations write as:

$$\begin{cases} \chi_{\alpha\beta} = d_{\alpha\beta\gamma\delta}M_{\delta\gamma}, & \text{(7a)} \\[2mm] \Gamma_{\alpha\beta\gamma} = h_{\alpha\beta\gamma\delta\epsilon\zeta}R_{\zeta\epsilon\delta}, & \text{(7b)} \end{cases}$$

where $(d_{\alpha\beta\gamma\delta})$ and $(h_{\alpha\beta\gamma\delta\epsilon\zeta})$ represent compliance tensors which are explicitly expressed in terms of the elastic components through the thickness of the plate (Sab and Lebée, 2015). $d_{\alpha\beta\gamma\delta}$ designates the classical bending compliance fourth-order tensor, inverse of the bending stiffness fourth-order tensor $D_{\alpha\beta\gamma\delta}$. Both tensors are positive definite and symmetric.

The generalized shear compliance tensor $h_{\alpha\beta\gamma\delta\epsilon\zeta}$ is symmetric and positive but it is definite only its image $\mathrm{Im}\,h$ whose dimension is between two and six, depending on the elastic properties of the plate. More details about the subspace $\mathrm{Im}\,h$ are given in Appendix A. The generalized shear stiffness tensor $(H_{\alpha\beta\gamma\delta\epsilon\zeta})$ is the Moore-Penrose pseudo inverse of $(h_{\alpha\beta\gamma\delta\epsilon\zeta})$. The Bending-Gradient equilibrium equations are given by:

$$\begin{cases} R_{\alpha\beta\gamma} - P^{S}_{\alpha\beta\gamma\delta\epsilon\zeta}M_{\zeta\epsilon,\delta} = 0, & \text{(8a)} \\[2mm] i_{\alpha\beta\gamma\delta}R_{\delta\gamma\beta,\alpha} + p = 0. & \text{(8b)} \end{cases}$$

where $P^{S}_{\alpha\beta\gamma\delta\epsilon\zeta}$ designates the orthogonal projection operator onto $\mathrm{Im}\,h$.

We note that, regardless of the positive definiteness of the shear compliance tensor $(h_{\alpha\beta\gamma\delta\epsilon\zeta})$, one can derive the conventional shear force $Q_{\alpha} = \langle\sigma_{\alpha3}\rangle$ from $R_{\alpha\beta\gamma}$ by:

$$Q_{\alpha} = R_{\alpha\beta\beta}. \tag{9}$$

Hence, equation (8)b can be restated as:

$$Q_{\alpha,\alpha} + p = 0. \tag{10}$$

3.3. Homogeneous plates

It was shown in Lebée and Sab (2015), Lebée and Sab (2015), Sab and Lebée (2015) that the Bending-Gradient theory cannot be reduced to a Reissner-Mindlin theory in general.

However, when the plate under consideration is homogeneous, the two theories coincide. In this case, the generalized shear tensor $(h_{\alpha\beta\gamma\delta\epsilon\zeta})$ can be expressed as:

$$h_{\alpha\beta\gamma\delta\epsilon\zeta} = i_{\alpha\beta\gamma\eta} f_{\eta\theta}^R i_{\theta\delta\varepsilon\zeta}, \tag{11}$$

where $(f_{\eta\theta}^R)$ is a positive definite symmetric second-order tensor called the Reissner-Mindlin shear compliance tensor. Furthermore, in this case, the generalized rotation tensor $(\Phi_{\alpha\beta\gamma})$ is of the form:

$$\Phi_{\alpha\beta\gamma} = i_{\alpha\beta\gamma\delta}\varphi_\delta, \tag{12}$$

where (φ_δ) is a 2D vector representing rotations. The generalized shear force $(R_{\alpha\beta\gamma})$ can be as well expressed as:

$$R_{\alpha\beta\gamma} = \frac{2}{3} i_{\alpha\beta\eta\theta} M_{\theta\gamma,\gamma}.$$

It follows that equations (8) become:

$$\begin{cases} Q_\alpha - M_{\alpha\beta,\beta} = 0, & \text{(13a)} \\ Q_{\alpha,\alpha} + p = 0, & \text{(13b)} \end{cases}$$

which constitute the well-known Reissner-Mindlin equilibrium equations.

3.4. Projection of the Bending-Gradient plate model

As previously mentioned, the Bending-Gradient theory is considered as an extension of the Reissner-Mindlin theory to laminated plates. It is hence interesting to try to approximate the Bending-Gradient model through an appropriate Reissner-Mindlin's model. In this section, we present two means to project the Bending-Gradient model on a Reissner-Mindlin model: the shear compliance projection (SCP) and the shear stiffness projection (SSP). These projections are discussed in full-detail in (Sab and Lebée, 2015).

3.4.1. The Shear Compliance Projection (SCP)

Consider a Bending-Gradient model with shear compliance tensor $(h_{\alpha\beta\gamma\delta\epsilon\zeta})$ and let $(f_{\alpha\beta}^{\mathrm{RM}})$ denote the corresponding Reissner-Mindlin compliance. The first approach consists in con-

sidering the following projection of $(h_{\alpha\beta\gamma\delta\epsilon\zeta})$:

$$\begin{cases} f_{11}^{\mathrm{RM}} = \dfrac{4}{9}\left(h_{111111} + h_{122221} + 2h_{111221}\right), \\[2mm] f_{12}^{\mathrm{RM}} = f_{21}^{\mathrm{RM}} = \dfrac{4}{9}\left(h_{111121} + h_{111222} + h_{121221} + h_{222221}\right), \\[2mm] f_{22}^{\mathrm{RM}} = \dfrac{4}{9}\left(h_{222222} + h_{121121} + 2h_{121222}\right). \end{cases} \quad (14)$$

This projection is equivalent to assuming $R_{\alpha\beta\gamma} = \frac{2}{3} i_{\alpha\beta\gamma\eta} Q_\eta$ in the expression of the Bending-Gradient shear stress energy density (Sab and Lebée, 2015).

In the framework of this projection, an evaluation of the distance between the Bending-Gradient plate model and the Reissner-Mindlin model was suggested (Lebée and Sab (2011), Lebée and Sab (2011)). Indeed, when the plate is homogeneous, the distance between the two models is equal to zero.

3.4.2. The Shear Stiffness Projection (SSP)

We now study the Shear Stiffness Projection which consists in supposing that the Reissner-Mindlin's shear stiffness tensor $(F_{\alpha\beta}^{\mathrm{RM}})$ associated to the Bending-Gradient shear stiffness tensor $(H_{\alpha\beta\gamma\delta\epsilon\zeta})$ is of the form:

$$\begin{cases} F_{11}^{\mathrm{RM}} = H_{111111} + H_{122221} + 2H_{111221}, \\[2mm] F_{12}^{\mathrm{RM}} = F_{21}^{\mathrm{RM}} = H_{111121} + H_{111222} + H_{121221} + H_{222221}, \\[2mm] F_{22}^{\mathrm{RM}} = H_{222222} + H_{121121} + 2H_{121222}. \end{cases} \quad (15)$$

Using this projection is equivalent to assuming that the generalized rotation is of the form $\Phi_{\alpha\beta\gamma} = i_{\alpha\beta\gamma\delta} \varphi_\delta$ in the expression of the Bending-Gradient shear strain energy density (Sab and Lebée, 2015), where (φ_δ) is a Reissner-Mindlin rotation vector.

It should be strongly emphasized that, unless for homogeneous plates, the shear stiffness projection and the shear compliance projection lead to different approximations. Hence, $(F_{\alpha\beta}^{\mathrm{RM}})$ is not the inverse of $(f_{\alpha\beta}^{\mathrm{RM}})$ in the general case (Sab and Lebée, 2015).

3.5. Kelvin Notations

Expressing the Bending-Gradient equations involves tensors with up to six indices which can be somehow cumbersome. This is why we introduce in this section Kelvin notation

which allows us to express any order tensor in the form of a matrix. Contractions products are hence turned into conventional matrix products. In the following, brackets $[\bullet]$ are used to denote that a tensor is considered in a matrix form. Thus, $[\bullet]$ is a linear operator reallocating tensor components. For example, the bending moment $(M_{\alpha\beta})$ and the curvature tensor $(\chi_{\alpha\beta})$ can be expressed as:

$$[M] = \begin{bmatrix} M_{11} \\ M_{22} \\ \sqrt{2}M_{12} \end{bmatrix}, \quad [\chi] = \begin{bmatrix} \chi_{11} \\ \chi_{22} \\ \sqrt{2}\chi_{12} \end{bmatrix}. \tag{16}$$

The fourth-order tensor $(D_{\alpha\beta\gamma\delta})$ is obtained through:

$$[D] = \left\langle x_3^2 \left[C^\sigma\right] \right\rangle, \tag{17}$$

where $C_{\alpha\beta\gamma\delta}^\sigma = C_{\alpha\beta\gamma\delta} - \dfrac{C_{\alpha\beta33}C_{\gamma\delta33}}{C_{3333}}$ corresponds to the plane stress stiffness. $[D]$ and $[C^\sigma]$ take the following matrix form:

$$[D] = \begin{bmatrix} D_{1111} & D_{2211} & \sqrt{2}D_{1211} \\ D_{2211} & D_{2222} & \sqrt{2}D_{1222} \\ \sqrt{2}D_{1211} & \sqrt{2}D_{1222} & 2D_{1212} \end{bmatrix}. \tag{18}$$

The constitutive equation $M_{\alpha\beta} = D_{\alpha\beta\gamma\delta} : \chi_{\delta\gamma}$ becomes a vector-matrix product:

$$[M] = [D] \cdot [\chi]. \tag{19}$$

Shear static unknowns are reallocated in a vector form as:

$$[R] = \begin{bmatrix} R_{111} \\ R_{221} \\ \sqrt{2}R_{121} \\ R_{112} \\ R_{222} \\ \sqrt{2}R_{122} \end{bmatrix}, \quad [\Gamma] = \begin{bmatrix} \Gamma_{111} \\ \Gamma_{221} \\ \sqrt{2}\Gamma_{121} \\ \Gamma_{112} \\ \Gamma_{222} \\ \sqrt{2}\Gamma_{122} \end{bmatrix}, \quad [\Phi] = \begin{bmatrix} \Phi_{111} \\ \Phi_{221} \\ \sqrt{2}\Phi_{121} \\ \Phi_{112} \\ \Phi_{222} \\ \sqrt{2}\Phi_{122} \end{bmatrix}. \tag{20}$$

The third-order tensor $(i_{\alpha\beta\gamma\delta}U_{3,\delta})$ is expressed in Kelvin notation by:

$$[i \cdot \nabla U_3] = U_{3,1} \left[J^1\right] + U_{3,2} \left[J^2\right], \tag{21}$$

10

where

$$[J^1]^T = \left[1, 0, 0, 0, 0, \frac{1}{\sqrt{2}}\right], \quad [J^2]^T = \left[0, 0, \frac{1}{\sqrt{2}}, 0, 0, 1\right]. \tag{22}$$

The Bending-Gradient shear compliance and stiffness tensors $(h_{\alpha\beta\gamma\delta\epsilon\zeta})$ and $(H_{\alpha\beta\gamma\delta\epsilon\zeta})$ are turned into a 6×6-matrix:

$$[h] = \begin{bmatrix} h_{111111} & h_{111122} & \sqrt{2}h_{111121} & h_{111211} & h_{111222} & \sqrt{2}h_{111221} \\ h_{221111} & h_{221122} & \sqrt{2}h_{221121} & h_{221211} & h_{221222} & \sqrt{2}h_{221221} \\ \sqrt{2}h_{121111} & \sqrt{2}h_{121122} & 2h_{121121} & \sqrt{2}h_{121211} & \sqrt{2}h_{121222} & 2h_{121221} \\ h_{112111} & h_{112122} & \sqrt{2}h_{112121} & h_{112211} & h_{112222} & \sqrt{2}h_{112221} \\ h_{222111} & h_{222122} & \sqrt{2}h_{222121} & h_{222211} & h_{222222} & \sqrt{2}h_{222221} \\ \sqrt{2}h_{122111} & \sqrt{2}h_{122122} & 2h_{122121} & \sqrt{2}h_{122211} & \sqrt{2}h_{122222} & 2h_{122221} \end{bmatrix}. \tag{23}$$

Note that we use the same letter for tensor and matrix components. However, two indices represent matrix components whereas six indices designate tensor components. For instance, h_{221121} is the tensor component of $(h_{\alpha\beta\gamma\delta\epsilon\zeta})$ whereas $h_{23} = \sqrt{2}h_{221121}$ is the matrix component of $[h]$.

As already indicated, the shear compliance tensor $h_{\alpha\beta\gamma\delta\epsilon\zeta}$ is not always invertible. A new feature of our work is the reduction method, presented and detailed thereafter, in order to calculate the shear stiffness tensor.

3.6. The reduction method

The reduction method consists in introducing the constraint $(\Phi_{\alpha\beta\gamma}) \in \operatorname{Im} h$ when the dimension of $\operatorname{Im} h$ is strictly lower than six (see Appendix A). The first step consists in computing the pseudo inverse $(H_{\alpha\beta\gamma\delta\epsilon\zeta})$ through the Singular Value decomposition (SVD). Accordingly, the real-valued compliance matrix $[h]$ is factored into:

$$[h] = [N] \cdot [a] \cdot [N]^T, \tag{24}$$

where $[a]$ is a 6×6 diagonal matrix:

$$[a] = \begin{bmatrix} a_1 & 0 & 0 & 0 & 0 & 0 \\ 0 & a_2 & 0 & 0 & 0 & 0 \\ 0 & 0 & a_3 & 0 & 0 & 0 \\ 0 & 0 & 0 & a_4 & 0 & 0 \\ 0 & 0 & 0 & 0 & a_5 & 0 \\ 0 & 0 & 0 & 0 & 0 & a_6 \end{bmatrix}, \tag{25}$$

and $[N]$ is an orthogonal 6×6 matrix with $[N]^T = [N]^{-1}$, where $[N]^T$ denotes the transpose of $[N]$.

The Moore-Penrose pseudo inverse $(H_{\alpha\beta\gamma\delta\epsilon\zeta})$ is hence obtained through:

$$[H] = [N] . [A] . [N]^T = [N] . \begin{bmatrix} A_1 & 0 & 0 & 0 & 0 & 0 \\ 0 & A_2 & 0 & 0 & 0 & 0 \\ 0 & 0 & A_3 & 0 & 0 & 0 \\ 0 & 0 & 0 & A_4 & 0 & 0 \\ 0 & 0 & 0 & 0 & A_5 & 0 \\ 0 & 0 & 0 & 0 & 0 & A_6 \end{bmatrix} . [N]^T, \tag{26}$$

with $A_k = 0$ if $a_k = 0$ and $A_k = \frac{1}{a_k}$ if $a_k \neq 0$.

Sab and Lebée (2015) demonstrated that the projection operator $(P^S_{\alpha\beta\gamma\delta\epsilon\zeta})$ can be expressed in the form of a matrix as:

$$\left[P^S\right] = [H] \cdot [h] = [h] \cdot [H]. \tag{27}$$

Substituting $[h]$ and $[H]$ by their expressions (24) and (26), we obtain that:

$$\left[P^S\right] = [N] . [\alpha] . [N]^T = [N] . \begin{bmatrix} \alpha_1 & 0 & 0 & 0 & 0 & 0 \\ 0 & \alpha_2 & 0 & 0 & 0 & 0 \\ 0 & 0 & \alpha_3 & 0 & 0 & 0 \\ 0 & 0 & 0 & \alpha_4 & 0 & 0 \\ 0 & 0 & 0 & 0 & \alpha_5 & 0 \\ 0 & 0 & 0 & 0 & 0 & \alpha_6 \end{bmatrix} . [N]^T, \tag{28}$$

where $\alpha_k = 0$ if $a_k = 0$ and $\alpha_k = 1$ if $a_k \neq 0$. In practice, assuming α_k are sorted in decreasing order, if $\alpha_k \leq 10^{-3}\alpha_1$, then $\alpha_k = 0$.

Let $(P^K_{\alpha\beta\gamma\delta\epsilon\zeta})$ denote the projection operator onto $\mathrm{Ker}\, h$ (see Appendix A). $(P^K_{\alpha\beta\gamma\delta\epsilon\zeta})$ has the following form:

$$
[P^K] = [N].[\beta].[N]^T = [N].
\begin{bmatrix}
\beta_1 & 0 & 0 & 0 & 0 & 0 \\
0 & \beta_2 & 0 & 0 & 0 & 0 \\
0 & 0 & \beta_3 & 0 & 0 & 0 \\
0 & 0 & 0 & \beta_4 & 0 & 0 \\
0 & 0 & 0 & 0 & \beta_5 & 0 \\
0 & 0 & 0 & 0 & 0 & \beta_6
\end{bmatrix}
.[N]^T,
\tag{29}
$$

where $\beta_k = 1$ if $a_k = 0$ and $\beta_k = 0$ if $a_k \neq 0$.

As stated earlier, the condition $\Gamma_{\alpha\beta\gamma} \in \mathrm{Im}\, h$ is equivalent to $\Phi_{\alpha\beta\gamma} \in \mathrm{Im}\, h$ since $i_{\alpha\beta\gamma\delta}U_{3,\delta}$ always belongs to $\mathrm{Im}\, h$. This implies that

$$
[P^K] \cdot [\Phi] = [P^K] \cdot [\Gamma],
\tag{30}
$$

and

$$
[P^K] \cdot [i \cdot \nabla U_3] = 0.
\tag{31}
$$

Combining equations (7)b, (29) and (30) yields:

$$
[P^K] \cdot [\Phi] = [P^K] \cdot [\Gamma] = [N] \cdot [\beta] \cdot [N]^T \cdot [N] \cdot [\alpha] \cdot [N]^T \cdot [R] = 0
\tag{32}
$$

since we have that:

$$
[N] \cdot [N]^T = [I] \quad \text{and} \quad [\beta] \cdot [\alpha] = 0.
\tag{33}
$$

Introducing the change of variable $[\Phi] = [N] \cdot [\Phi^*]$ in equation (32) grants:

$$
[P^K] \cdot [\Phi] = [N] \cdot [\beta] \cdot [N]^T \cdot [\Phi] = [N] \cdot [\beta] \cdot [\Phi^*] = 0 \iff [\beta] \cdot [\Phi^*] = 0,
\tag{34}
$$

which means that $(\Phi_{\alpha\beta\gamma}) \in \mathrm{Im}\, h$ if, and only if, $\Phi^*_i = 0$ for all i such that $a_i = 0$.

In brief, the reduction method consists in making the change of variable

$$
[\Phi] = [N] \cdot [\Phi^*]
\tag{35}
$$

13

in the Bending-Gradient equations (5), (7) and (8), and imposing $\Phi_i^* = 0$ for all i such that $a_i = 0$. This allows us to write the reciprocal relationship of equation (7)b:

$$R_{\alpha\beta\gamma} = H_{\alpha\beta\gamma\delta\epsilon\zeta}\Gamma_{\zeta\epsilon\delta}, \quad \Gamma_{\alpha\beta\gamma} \in \operatorname{Im} h. \tag{36}$$

4. Propagation of plane waves in an anisotropic plate

In this section, we first study the propagation of waves in anisotropic plates in the framework of the three-dimensional elasticity theory. Our main purpose is to accurately predict the dispersion curve associated to long flexural waves, which is conventionally approximated by the finite element method.

Good approximations of the static 3D solutions can be obtained from the Bending-Gradient plate model (Sab and Lebée, 2015). It is hence worth to also estimate the dispersion relation through the Bending-Gradient equations of motion. We also suggest using the Reissner-Mindlin models obtained by projections of the Bending-Gradient model as explained in Section 3.4.

In this part, we consider a symmetrical plate with the same configuration as Section 3. Assuming the plate is infinite in directions 1 and 2, no boundary conditions need to be applied on ∂V_{lat}. We particularly focus attention on waves propagating in direction 1.

4.1. Exact dispersion curves for guided waves

4.1.1. Three-dimensional equations of motion

For plane waves propagating in direction 1, the displacement vector u_i is a function of the coordinates (x_1, x_3) and of the time t:

$$u_i = u_i(x_1, x_3, t), \quad i = 1, 2, 3.$$

The basic equation of motion is obtained by relating the stress σ_{ij} to the motion of the particles in the plate using Newton's second law. Let ρ denote the density (mass per unit volume). In the absence of body forces, the Momentum equation writes:

$$\sigma_{ij,j} - \rho\ddot{u}_i = 0, \tag{37}$$

14

where the double dot indicates a second derivative with respect to time $\left(\ddot{x} = \frac{dx^2}{dt^2}\right)$.

Wave propagation in infinite anisotropic elastic plate is governed by the full set of equations of the three-dimensional theory of elasticity, namely:

$$
\begin{cases}
\sigma_{ij,j} - \rho \ddot{u}_i = 0, & \text{(38a)} \\[2mm]
\sigma_{ij} - C_{ijkl}(x_3) : \varepsilon_{lk} = 0, & \text{(38b)} \\[2mm]
\varepsilon_{ij} - \dfrac{1}{2}(u_{i,j} + u_{j,i}) = 0, & \text{(38c)} \\[2mm]
\sigma_{i3} = 0 \ \text{ at } x_3 = \pm\dfrac{h}{2}. & \text{(38d)}
\end{cases}
$$

Additionally, the stresses σ_{i3} and the displacements u_i must be continuous at the interfaces between the different layers of the plate.

For harmonic waves propagating in direction 1 at time t, the displacements u_i, solution to (38), can be described using:

$$
u_i(x_1, x_3, t) = \Re\left(\hat{u}_i(x_3) e^{j(\omega t - kx_1)}\right), \quad i = 1, 2, 3, \tag{39}
$$

where $(\hat{u}_i)_{i=1,2,3}$ are amplitudes of the displacement components, ω is the angular frequency, $k \neq 0$ is the wave number and j the imaginary unit. The symbol $\Re(z)$ is used to designate the real part of the complex number z. We denote by λ the wavelength and c the wave velocity. We recall that the wave number is related to the wavelength through:

$$
k = \frac{2\pi}{\lambda}, \tag{40}
$$

and that the phase velocity c is expressed as:

$$
c = \frac{\omega}{k}. \tag{41}
$$

The problem is to find a relation between the angular frequency ω and the wave number k which ensures the existence of a non-zero vector $(\hat{u}_i)_{i=1,2,3}$, satisfying the three-dimensional equations of motion (38).

Reference solutions of the 3D problem (38) can be computed via the finite element method whose procedure is presented next.

4.1.2. Resolution by means of Finite Element Analysis

Injecting the plane wave displacement (39) in the local equations (38) leads to the formulation of a quadratic eigenvalue problem in both wavenumber k and frequency ω that has to be solved. In the case of homogeneous isotropic plates, it can be reduced to the well known Lamb modes transcendental equation (Lamb, 1917). The case of laminated plates has been first investigated by T. Thomson (1950), who expressed the inter-lamina continuity conditions with the help of *transfer matrices*. As a consequence of the numerical instability of the method (Haskell, 1953), several reformulations has been proposed in the following decades (Schmidt and Tango, 2007, Nayfeh, 1991, Rokhlin and Wang, 2002).

Alternatively, the variationnal formulation of the problem (integral equations) can be used (Dong and B. Nelson, 1972, Datta et al., 1988, Xi et al., 2000). The finite element approach then leads to the following eigenvalue problem:

$$\left(k^2 \left[K_2 \right] + jk \left[K_1 \right] + \left[K_0 \right] - \omega^2 \left[\mathbb{M} \right] \right) \left[\mathbb{U} \right] = \underline{\mathbf{0}} , \tag{42}$$

where $[K_i]$, $i = 1, 2, 3$ and $[\mathbb{M}]$ are symetric hermitian matrices and $[\mathbb{U}]$ is the vector of nodal displacements. This formulation is usually referred as the Spectral Finite Element Method (J. Shorter, 2004, Barbieri et al., 2009) (SFEM) or Semi-Analytical Finite Element method (Bartoli et al., 2006) (SAFE). The preceding eigenvalue problem is solved more easily by searching the eigenfrequencies related to a given wavenumber. However, it is often more convenient to search for the wavenumber solutions corresponding to a fixed frequency; this can be performed by the resolution of the associated quadratic eigenvalue problem, giving both real and imaginary solutions (resp. denoting propagating and evanescent waves).

This method has been implemented here to compute reference solutions to the problem of wave propagation in anisotropic plates. Linear elements were used since the problem is one-dimensional in x_3. We used three degrees of freedom per node to take account of the three components of the displacement field. In the wavelength range of interest, it has been observed that 10 elements by layer was sufficient to avoid convergence issues.

4.2. Plate models dispersion curves

4.2.1. Bending-Gradient equations of motion

In this section, we study wave propagation in anisotropic media using the Bending-Gradient model. We first provide the formulation of the Bending-Gradient equations of motion for heterogeneous plates. Then, we explain how to find numerically the corresponding dispersion curves. Finally, the classical dispersion relation for the Reissner-Mindlin and the Kirchhoff-Love model are retrieved.

The formulation of the wave propagation problem is based on Mindlin's paper (Mindlin, 1951), in which a comparison was made between the exact solution of the three-dimensional equations and the solution obtained using the CPT. It was shown that the CPT deviates significantly from the three-dimensional theory whether the rotatory inertia correction is added or not. However, when taking into consideration the effects of transverse shear deformation solely, the obtained solution is very close to the three-dimensional solution. Thereby, the Bending-Gradient equations of motion are formulated by considering that the only inertia forces are those due to the transverse translation of the plate elements, and hence neglecting rotatory effects. In this case, the transverse load p given by:

$$p = -\ddot{U}_3 \bar{\rho}, \tag{43}$$

where $\bar{\rho} = \langle \rho \rangle$. In the following, we assume that the shear compliance tensor $h_{\alpha\beta\gamma\delta\varepsilon\zeta}$ is definite. In this case, $P^S_{\alpha\beta\gamma\delta\varepsilon\zeta}$ is the identity operator. Hence, the generalized shear force $R_{\alpha\beta\gamma}$ is the gradient of the bending moment $M_{\alpha\beta}$.

Wave propagation in anisotropic plates in the absence of body forces is thus modelled by:

$$\begin{cases} R_{\alpha\beta\gamma} - M_{\alpha\beta,\gamma} = 0, \\ Q_\alpha = R_{\alpha\beta\beta}, \\ Q_{\alpha,\alpha} = \ddot{U}_3 \bar{\rho}. \end{cases} \tag{44}$$

Using constitutive equations (7) and compatibility conditions (5), equations (44) are restated in terms of the generalized displacements $(U_3, \Phi_{\alpha\beta\gamma})(x_1, t)$ as:

$$\begin{cases} H_{\alpha\beta\gamma\delta\epsilon\zeta} \left(\Phi_{\zeta\epsilon\delta} + i_{\zeta\epsilon\delta\eta} U_{3,\eta} \right) - D_{\alpha\beta\theta\epsilon} \Phi_{\epsilon\theta\xi,\xi\gamma} = 0, \tag{45a} \\ H_{\alpha\beta\beta\delta\epsilon\zeta} \left(\Phi_{\zeta\epsilon\delta,\alpha} + i_{\zeta\epsilon\delta\eta} U_{3,\eta\alpha} \right) = \ddot{U}_3 \bar{\rho}. \tag{45b} \end{cases}$$

17

We point out that when the sixth-order tensor $h_{\alpha\beta\gamma\delta\varepsilon\zeta}$ is not definite, it suffices to make the change of variables (35) in equations (45) as detailed in Sect. 3.6.

For waves propagating in direction 1, the generalized displacements $(U_3, \Phi_{\alpha\beta\gamma})(x_1, t)$, solution to (45), can be described using:

$$\begin{cases} U_3(x_1, t) = \Re\left(\hat{U}_3 e^{j(\omega t - kx_1)}\right), & \text{(46a)} \\ \Phi_{\alpha\beta\gamma}(x_1, t) = \Re\left(\hat{\Phi}_{\alpha\beta\gamma} e^{j(\omega t - kx_1)}\right), & \text{(46b)} \end{cases}$$

where $\hat{U}_3$ and $\hat{\Phi}_{\alpha\beta\gamma}$ are arbitrary constants. Indeed, all derivatives with respect to x_2 are equal to zero, since the displacements U_3 and $\Phi_{\alpha\beta\gamma}$ are functions of x_1. Thus, substituting (46) into (45) yields:

$$\begin{cases} H_{\alpha\beta\gamma\delta\epsilon\zeta}\left(\hat{\Phi}_{\zeta\epsilon\delta} - jki_{\zeta\epsilon\delta1}\hat{U}_3\right) + k^2 D_{\alpha\beta\theta\epsilon}\hat{\Phi}_{\epsilon\theta1}\delta_{1\gamma} = 0, & \text{(47a)} \\ H_{1\beta\beta\delta\epsilon\zeta}\left(-jk\hat{\Phi}_{\zeta\epsilon\delta} - k^2 i_{\zeta\epsilon\delta1}\hat{U}_3\right) + \omega^2 \hat{U}_3 \bar{\rho} = 0. & \text{(47b)} \end{cases}$$

Finding the dispersion relation associated to flexural waves requires using a mathematical computing software such as Matlab. The implementation of equations (47) is presented in the following section.

4.2.2. Implementation of plate dispersion equations

Suppose that the shear compliance tensor $h_{\alpha\beta\gamma\delta\epsilon\zeta}$ is definite. Using Kelvin notation introduced in Section 3.5, equation (44)a writes:

$$[R] - [M \otimes \nabla] = 0, \tag{48}$$

where $[M \otimes \nabla]$ represents the gradient of the bending moment expressed by:

$$[M \otimes \nabla] = \begin{bmatrix} M_{11,1} \\ M_{22,1} \\ \sqrt{2}M_{12,1} \\ 0 \\ 0 \\ 0 \end{bmatrix}. \tag{49}$$

Using compatibility conditions (5)b, $[R]$ is defined by:

$$[R] = [H] \cdot ([\Phi] + [i \cdot \nabla U_3]) \,. \tag{50}$$

The third-order tensor $[i \cdot \nabla U_3]$ is expressed in Kelvin notation by:

$$[i \cdot \nabla U_3] = U_{3,1} [J^1] = -jk\hat{U}_3 [J^1] \,. \tag{51}$$

Using compatibility conditions (5)a, we have:

$$\begin{bmatrix} M_{11,1} \\ M_{22,1} \\ \sqrt{2}M_{12,1} \end{bmatrix} = [D] \cdot \begin{bmatrix} \Phi_{111,11} \\ \Phi_{221,11} \\ \sqrt{2}\Phi_{121,11} \end{bmatrix} = -k^2 [D] \cdot \begin{bmatrix} \hat{\Phi}_{111} \\ \hat{\Phi}_{221} \\ \sqrt{2}\hat{\Phi}_{121} \end{bmatrix} \,. \tag{52}$$

Making use of the notations described above, wave propagation equations (47) can be written as a matrix-vector product:

$$[\mathcal{A}] \cdot [\delta] = 0, \tag{53}$$

where $[\delta]$ is a vector representing the generalized displacements $\left(\hat{U}_3, \hat{\Phi}_{\alpha\beta\gamma} \right)$:

$$[\delta]^T = \left[\hat{U}_3, \hat{\Phi}_{111}, \hat{\Phi}_{221}, \sqrt{2}\hat{\Phi}_{121}, \hat{\Phi}_{112}, \hat{\Phi}_{222}, \sqrt{2}\hat{\Phi}_{122} \right], \tag{54}$$

and $[\mathcal{A}]$ is a symmetric 7×7 matrix given by:

$$[\mathcal{A}] = \begin{bmatrix} \mathcal{A}_{11} & \mathcal{A}_{12} & \mathcal{A}_{13} & \mathcal{A}_{14} & \mathcal{A}_{15} & \mathcal{A}_{16} & \mathcal{A}_{17} \\ \mathcal{A}_{12} & H_{11} + k^2 D_{11} & H_{12} + k^2 D_{12} & H_{13} + k^2 D_{13} & H_{14} & H_{15} & H_{16} \\ \mathcal{A}_{13} & H_{21} + k^2 D_{21} & H_{22} + k^2 D_{22} & H_{23} + k^2 D_{23} & H_{24} & H_{25} & H_{26} \\ \mathcal{A}_{14} & H_{31} + k^2 D_{31} & H_{32} + k^2 D_{32} & H_{33} + k^2 D_{33} & H_{34} & H_{35} & H_{36} \\ \mathcal{A}_{15} & H_{41} & H_{42} & H_{43} & H_{44} & H_{45} & H_{46} \\ \mathcal{A}_{16} & H_{51} & H_{52} & H_{53} & H_{54} & H_{55} & H_{56} \\ \mathcal{A}_{17} & H_{61} & H_{62} & H_{63} & H_{64} & H_{65} & H_{66} \end{bmatrix}, \tag{55}$$

with

$$
\begin{cases}
\mathcal{A}_{11} = \omega^2 \bar{\rho} - k^2 \left(H_{11} + \sqrt{2} H_{61} + \frac{1}{2} H_{66} \right), \\[2mm]
\mathcal{A}_{12} = -jk \left(H_{11} + \frac{\sqrt{2}}{2} H_{16} \right), \\[2mm]
\mathcal{A}_{13} = -jk \left(H_{12} + \frac{\sqrt{2}}{2} H_{26} \right), \\[2mm]
\mathcal{A}_{14} = -jk \left(H_{13} + \frac{\sqrt{2}}{2} H_{36} \right), \\[2mm]
\mathcal{A}_{15} = -jk \left(H_{14} + \frac{\sqrt{2}}{2} H_{46} \right), \\[2mm]
\mathcal{A}_{16} = -jk \left(H_{15} + \frac{\sqrt{2}}{2} H_{56} \right), \\[2mm]
\mathcal{A}_{17} = -jk \left(H_{16} + \frac{\sqrt{2}}{2} H_{66} \right).
\end{cases}
\tag{56}
$$

The existence of non-trivial solutions to equation (53) implies the vanishing of the determinant of the square matrix $[\mathcal{A}]$:

$$
\det[\mathcal{A}] = 0.
\tag{57}
$$

Our aim is to find the expression of the angular frequency ω in terms of the wave number k which is purely real since it is associated to flexural waves. The analytical expression of the determinant of $[\mathcal{A}]$, being very lengthy, is omitted here. Nevertheless, it can be noticed that $\det[\mathcal{A}]$ is a second degree polynomial in ω of the form $a\omega^2 + b$, where a and b are functions of the wave number k. Therefore, equation (57) admits only two roots whose nature is determined by the sign of the quantity $-\dfrac{b}{a}$. It appears through numerical calculations using Matlab that the quantity $-\dfrac{b}{a}$ is always positive, and that the two roots of equation (57) are purely real and correspond to the forward and backward flexural waves.

We shall not go into details concerning the case when $h_{\alpha\beta\gamma\delta\epsilon\zeta}$ is not definite, but we note that the dispersion relation is obtained by setting to zero the determinant of a $(m+1)\times(m+1)$ matrix, where m denotes the dimension of $\operatorname{Im} h$, with $2 < m < 6$. For calculation and implementation details in the case of a single layer of anisotropic material, the reader is

referred to Appendix A.

For ease of computing the Bending-Gradient flexural dispersion curves, a code was created using the Matlab programming language. Kindly refer to Bejjani (2019) for further details. The code is simple to use in the sense that it provides the desired results just by inputting the constitutive material properties.

4.2.3. Reissner-Mindlin and Kirchhoff-Love plate models

Let us recall that when the Bending-Gradient shear compliance tensor $h_{\alpha\beta\gamma\delta\epsilon\zeta}$ is of the form (11), the Bending-Gradient model is turned into the Reissner-Mindlin model with $f_{\alpha\beta}^{\mathrm{R}}$ as shear forces compliance. In this case the flexural branches of the dispersion curve may be written as (see Appendix A):

$$\omega = \pm k \sqrt{\frac{k^4 F_{11}^{\mathrm{R}} \left(D_{1111} D_{2121} - D_{1121}^2\right) + k^2 D_{1111} \left(F_{11}^{\mathrm{R}} F_{22}^{\mathrm{R}} - (F_{12}^{\mathrm{R}})^2\right)}{\bar{\rho} \left(\left(F_{11}^{\mathrm{R}} + k^2 D_{1111}\right) \left(F_{22}^{\mathrm{R}} + k^2 D_{2121}\right) - \left(F_{12}^{\mathrm{R}} + k^2 D_{2111}\right)^2\right)}}. \tag{58}$$

where $F_{\alpha\beta}^{\mathrm{R}}$ is the shear stiffness tensor, inverse of the shear compliance tensor $f_{\alpha\beta}^{\mathrm{R}}$.

Finally, the Kirchhoff-Love theory is obtained setting $h_{\alpha\beta\gamma\delta\epsilon\zeta} = 0$. This leads to the classical result:

$$\omega = \pm \sqrt{\frac{D_{1111}}{\bar{\rho}}} k^2. \tag{59}$$

5. Numerical Results and Verification

Having presented the wave propagation problem and the derivation of its solution, we are now in position to evaluate the effectiveness of the Bending-Gradient theory and of the shear compliance and shear stiffness projections. Generally, this evaluation is performed by comparing obtained results to reference results. The natural reference for such an assessment is the solution of the three-dimensional dynamic problem, which can be computed using the finite element method (FEM) as detailed in Section 4.1.2. In the following, reference results are compared to those obtained using the Classical Plate Theory (CPT), the Bending-Gradient theory (BG) as well as the Shear Compliance (SCP), the Shear Stiffness (SSP) projections and the first order shear deformation theory ($\frac{\pi^2}{12}$-FOSDT).

Simulations reported in the present paper were performed using the calculation software Matlab. The proposed numerical method applies to any stack of layers whether the shear compliance tensor is definite or not. If the latter is the case, the reduction method presented in Section 3.6 is used in the calculations.

The analytical models presented throughout this work were applied to various laminate configurations. Below we present numerical simulations realized for a laminate whose material properties are listed in table 1 (Lebée and Sab, 2015, Pagano, 1969):

Table 1: Elastic properties of the laminate, E and G in Pa, ρ in kg/m^3

E_L	$E_N = E_T$	$G_{LN} = G_{LT}$	G_{TN}	$\nu_{LN} = \nu_{LT} = \nu_{TN}$	ρ
1.72e+11	6.89e+09	3.45e+09	2.75e+09	0.25	2260

The symbols E, G, ν and ρ respectively denote the Young's modulus, the shear modulus, Poisson's ratio and the density of the material. The indices L, T and N correspond respectively to the longitudinal, transversal and normal directions. Each ply of the laminate is made of unidirectional fiber-reinforced material oriented at θ relative to the bending direction x_1. All plies have the same thickness $h = 0.01$ mm and are perfectly bounded. In the following, symmetric laminates are designated by the sequence of fiber orientations, from the outermost ply till the midplane, enclosed by brackets subscripted with an s. For instance $[0°, 90°]_s$ denotes a 4-ply laminate with $[0°, 90°, 90°, 0°]$.

In the figures below, the x-axis indicates the thickness-wavelength ratio (h/λ). The y-axis corresponds to the ratio (c/c_S), where c is the wave velocity and c_S denotes a normalization factor defined by Mindlin (1951):

$$c_S = \sqrt{\frac{G_{LN}}{\rho}}.$$

In Figs. 2, 3 and 4 are illustrated the dispersion curves for a $[0°, 90°]_s$ ply, a $[-30°, 30°]_s$ ply and a $[0°, -45°, 90°, 45°]_s$ ply respectively. We mention that the shear compliance tensor $h_{\alpha\beta\gamma\delta\epsilon\zeta}$ of both 4-layer laminates is not definite and that the dimension of $\text{Im} \, h$ is equal to
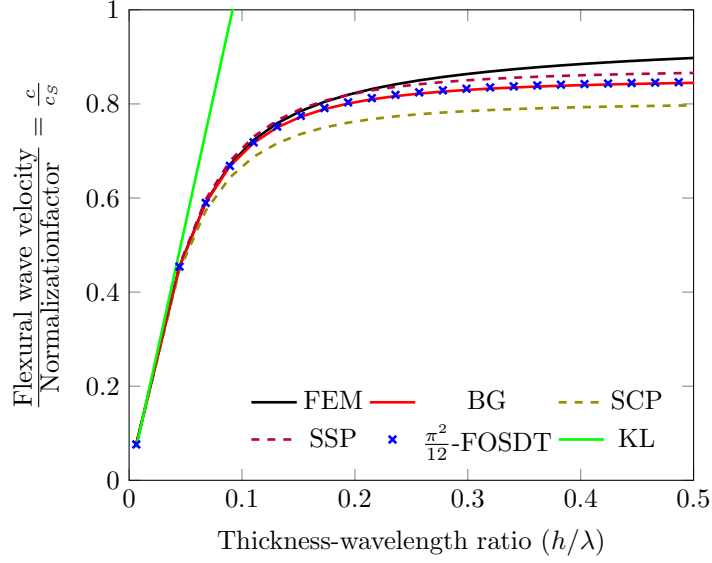
22

Figure 2: Comparison of the dispersion curves for a $[0°, 90°]_s$ ply

4. However, when considering the 8-layer laminate, the sixth-order tensor $h_{\alpha\beta\gamma\delta\epsilon\zeta}$ is definite and therefore $\dim \operatorname{Im} h = 6$.

The relative error is computed as follows:

$$\mathcal{E}_r = \frac{c_{app} - c_{fem}}{c_{fem}}, \tag{60}$$

where c_{app} and c_{fem} respectively denote the approximate value and the reference value of the the wave velocity. The relative errors with respect to reference solutions computed with the finite element method (FEM) are shown in Table 2 for a thickness-wavelength ratio $h/\lambda = 0.3$.

It is worth noting that dispersion relations generally depend on the angle of wave propagation ψ. Taking into account ψ in the computations consists in rotating the entire laminate by $-\psi$. In the following, calculations on the $[0°, -45°, 90°, 45°]_s$ ply are performed for several values of ψ ($+15°$, $+22°$ and $+45$) and the related relative errors are set out in Table 3.

As is seen from Figs. 2, 3 and 4, when the wavelength becomes less than 10 times the plate thickness, the Kirchhoff-Love theory (KL) fails to correctly predict the dispersion curve of the flexural mode. In fact, relative errors noticed for $h/\lambda = 0.3$ are greater than 80%. This is expected since the rotatory inertia and the transverse shear deformations are
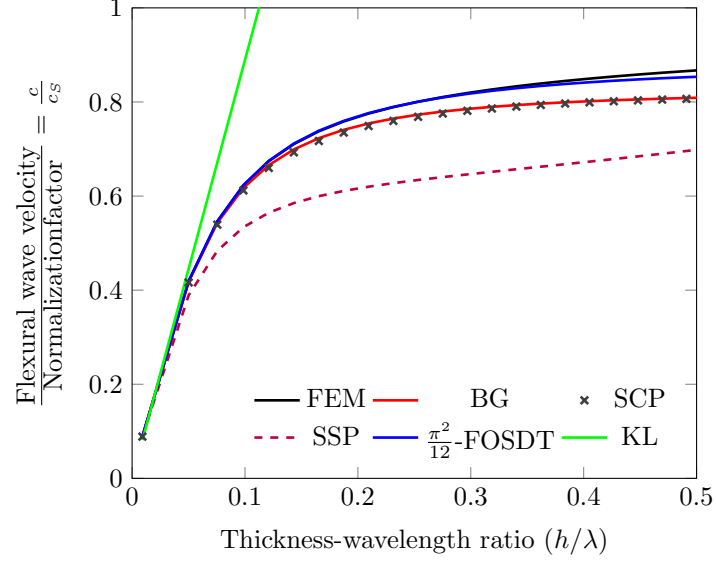
23

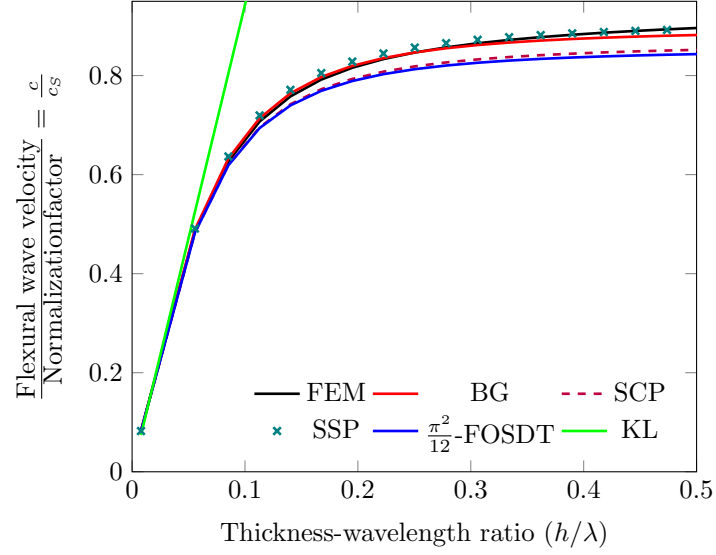Figure 3: Comparison of the dispersion curves for a $[-30°, 30°]_s$ ply

Figure 4: Comparison of the dispersion curves for a $[0°, -45°, 90°, 45°]_s$ ply

24

Table 2: Relative error of plate models compared to finite element results with $h/\lambda = 0.3$

Laminate	KL	$\frac{\pi^2}{12}$ FOSDT	BG	SCP	SSP
$[0°, 90°]_s$	1.044	-0.035	-0.038	-0.091	-0.015
$[-30°, 30°]_s$	0.896	-0.002	-0.041	-0.046	-0.211
$[0°, -45°, 90°, 45°]_s$	0.917	-0.045	-0.006	-0.037	0.008

Table 3: Relative error of plate models compared to finite element results for a $[0°, -45°, 90°, 45°]_s$ ply with $h/\lambda = 0.3$

ψ	KL	$\frac{\pi^2}{12}$ FOSDT	BG	SCP	SSP
$+15°$	0.935	-0.046	-0.005	-0.037	0.0029
$+22°$	0.960	-0.042	0.024	-0.036	0.005
$+45°$	1.064	0.0006	-0.024	-0.014	0.054

supposed to be negligible (Love, 1888).

In the case of a $[0°, 90°]_s$ ply, one can observe on Fig. 2 that the results obtained with the shear stiffness projection (SSP) agree well with the reference results (FEM). Indeed, the SSP wave velocity is lower than the reference value by 1.5% approximately. The Shear stiffness projection (SSP) is clearly more efficient than the shear compliance projection (SCP), which nevertheless gives a satisfactory approximation of the solution with an error $|\mathcal{E}_r|$ that does not exceed 9.1%.

When considering a $[-30°, 30°]_s$ ply, Fig. 3 shows a very good accordance between the shear compliance projection (SCP) and the finite element method (FEM). In this case, the shear stiffness projection (SSP) underestimates the dispersion curve of the flexural mode by 21.1%.

For the $[0°, -45°, 90°, 45°]_s$ ply, it is evidently seen on Fig. 4 that the curve obtained by the shear compliance (SCP) and the shear stiffness projections (SSP) match very well the solution computed with the finite element method (FEM). The relative error $|\mathcal{E}_r|$ has

a minimum value of 0.5% and a maximum value of 5% for both projections in case of all measurements (see Tables 2 and 3).

The conformity between the $\frac{\pi^2}{12}$-FOSDT and the reference results is very good according to Figs. 2, 3 and 4 with a relative error that reaches a maximum of about 4.6% in absolute value for the considered examples.

Tables 2 and 3 show that the the relative error $|\mathcal{E}_r|$ of the Bending-Gradient model ranges from 0.5% to 4.1%. Such small errors result in precise approximation of the wave dispersion relation, which is illustrated in Figs. 2, 3 and 4.

More numerical simulations were carried out to assess the validity range of the Bending-Gradient model and the Reissner-Mindlin models suggested in Section 3.4. For instance, we considered a multilayered plate consisting of alternate layers of the same thickness $h = 1\,\mathrm{mm}$ of epoxy-glass woven composite and aluminium whose elastic properties are respectively set down in Tables 4 and 5. The sequence is [GFRP, Al, GFRP, Al]$_s$ and the GFRP material directions L, N are aligned with Directions 1 and 2.

Table 4: Elastic properties of epoxy-glass fiber composite material Renno et al. (2013), E and G in Pa, ρ in kg/m^3

$E_L = E_T$	E_N	G_{LT}	$G_{LN} = G_{TN}$	ν_{LT}	$\nu_{LN} = \nu_{TN}$	ρ
5.40e+10	4.80e+09	3.16e+09	1.78e+09	0.06	0.31	2000

Table 5: Elastic properties of aluminium material Liu et al. (2016), E and G in Pa, ρ in kg/m^3

E	G	ν	ρ
7.20e+10	2.67e+10	0.35	2700

The obtained dispersion curves are depicted in Fig. 5. The relative errors with respect to finite element (FEM) solutions are given in Table 6 for a thickness-wavelength ratio $h/\lambda = 0.3$.
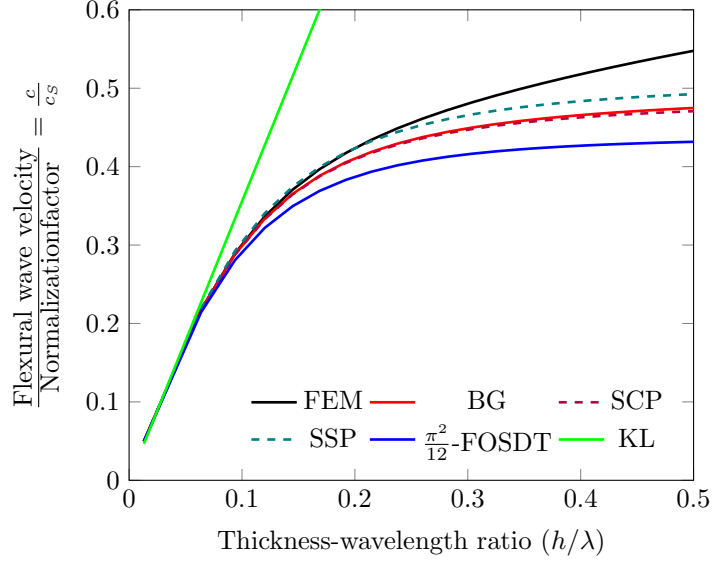
Figure 5: Comparison of the dispersion curves for a [GFRP, Al, GFRP, Al]$_s$ ply

Table 6: Relative error of plate models compared to finite element results with $h/\lambda = 0.3$ for a $[0°, 0°, 90°, 0°]_s$ ply

Laminate	$\frac{\pi^2}{12}$ FOSDT	BG	SCP	SSP
$[0°, 0°, 90°, 0°]_s$	-0.134	-0.065	-0.069	-0.031

According to Fig. 5, the agreement between the $\frac{\pi^2}{12}$-FOSDT and the reference results is poor. For a thickness-wavelength ratio $h/\lambda = 0.3$, the relative error $|\mathcal{E}_r|$ is around 13%.

It can be seen that the Bending-Gradient model (BG) and the shear compliance projection (SCP) provide good approximations of the flexural dispersion curves. The relative error $|\mathcal{E}_r|$ is lower than 7% as stated in Table 6.

The computed results reveal the better approximation from the shear stiffness projection (SSP) in this case. The relative error $|\mathcal{E}_r|$ is equal to 3.1% for $h/\lambda = 0.3$.

Whereas Reissner-Mindlin approximations (SCP, SSP, $\frac{\pi^2}{12}$-FOSDT) may give very accurate estimates of the dispersion curve in some specific cases, it appears that the Bending-Gradient approximation is the most robust one. Indeed, in all cases, reasonable estimates of the wave velocity is provided.

27

6. Conclusion

In this paper, we addressed the problem of flexural wave propagation in anisotropic laminated plates by using the Bending-Gradient theory. The Bending-Gradient problem was briefly recalled and two projections on a simplified Reissner-Mindlin model were introduced: the shear compliance projection and the shear stiffness projection. The particular case of homogeneous plates, in which the Bending-Gradient model is turned into a Reissner-Mindlin model, was also discussed.

Inspired by Mindlin's paper, the dynamic problem was formulated by taking into account transverse shear deformations and neglecting rotatory inertia effects. The solution of these equations enabled the derivation of the dispersion relation connecting the angular frequency and the wave number. The analytical models were verified by comparing them to finite element solutions considered as reference solutions. Numerical simulations were conducted and it was shown that the Reissner-Mindlin models obtained by projections may yield accurate estimations of the solution in some cases. Nevertheless, it was clear that the numerical results obtained by the Bending-Gradient theory are more robust and less sensitive to the ply configuration. Though the Bending-Gradient theory seems more complicated than the Reissner-Mindlin theory, a practical, easy-to-use and publicly accessible Matlab code was created for obtaining the Bending-Gradient flexural dispersion curves.

Appendix A.

A.1

Let $\underset{\approx}{\mathbb{R}}$ be the space of 2D third order tensors which comply with the following symmetries:

$$\underset{\approx}{\mathbb{R}} = \left\{ (X_{\alpha\beta\gamma}) \in \mathbb{R}^8 \mid X_{\alpha\beta\gamma} = X_{\beta\alpha\gamma} \right\}. \tag{A.1}$$

Sab and Lebée (2015) orthogonally decomposed the vector space $\underset{\approx}{\mathbb{R}}$, endowed with the scalar product $X_{\alpha\beta\gamma}X'_{\alpha\beta\gamma}$, into $\operatorname{Im} h$ and its orthogonal $\operatorname{Ker} h$:

$$\underset{\approx}{\mathbb{R}} = \operatorname{Ker} h \oplus \operatorname{Im} h,$$

where $\oplus$ is the direct sum operator (Section 2), $\text{Im}\, h$ is the image of the sixth-order shear force compliance tensor $h_{\alpha\beta\gamma\delta\epsilon\zeta}$:

$$\text{Im}\, h = \{h_{\alpha\beta\gamma\delta\varepsilon\zeta} X_{\zeta\varepsilon\delta}, \quad X_{\zeta\varepsilon\delta} \in \mathbb{R}\},$$

and $\text{Ker}\, h$ denotes its kernel:

$$\text{Ker}\, h = \{X_{\alpha\beta\gamma} \in \underset{\approx}{\mathbb{R}} \mid h_{\alpha\beta\gamma\delta\varepsilon\zeta} X_{\zeta\varepsilon\delta} = 0\}.$$

Sab and Lebée (2015) have proved that the shear force compliance tensor $h_{\alpha\beta\gamma\delta\epsilon\zeta}$ is definite only on the subspace $\text{Im}\, h$ whose dimension is between two and six, depending on the elastic properties of the plate. When the plate is homogeneous, the dimension of $\text{Im}\, h$ is exactly two and in this case the Bending-Gradient theory degenerates into the Reissner-Mindlin theory. When $h_{\alpha\beta\gamma\delta\epsilon\zeta}$ is definite and therefore invertible, $\text{Im}\, h$ is equal to $\underset{\approx}{\mathbb{R}}$ of dimension six.

A.2

For the particular case of homogeneous plates, we recall that the Bending-Gradient shear compliance tensor $h_{\alpha\beta\gamma\delta\epsilon\zeta}$ is of the form

$$h_{\alpha\beta\gamma\delta\epsilon\zeta} = i_{\alpha\beta\gamma\eta} f^R_{\eta\theta} i_{\theta\delta\varepsilon\zeta}. \tag{A.2}$$

Contracting three times the left and the right of both sides of the above equation with $\frac{2}{3} i_{\alpha\beta\gamma\delta}$, we obtain the expression of $f^R_{\alpha\beta}$ in terms of $h_{\alpha\beta\gamma\delta\epsilon\zeta}$:

$$\begin{cases} f^{\text{RM}}_{11} = \dfrac{4}{9} \left(h_{111111} + h_{122221} + 2h_{111221}\right), \\[2mm] f^{\text{RM}}_{12} = f^{\text{RM}}_{21} = \dfrac{4}{9} \left(h_{111121} + h_{111222} + h_{121221} + h_{222221}\right), \\[2mm] f^{\text{RM}}_{22} = \dfrac{4}{9} \left(h_{222222} + h_{121121} + 2h_{121222}\right). \end{cases} \tag{A.3}$$

In view of the positive definiteness of $f^R_{\alpha\beta}$, we define its inverse $F^R_{\alpha\beta}$.

Propagation of elastic waves is governed by the equations of the Bending-Gradient theory, which for homogeneous plates write:

$$\begin{cases} Q_\alpha - M_{\alpha\beta,\beta} = 0, \\[2mm] Q_{\alpha,\alpha} = \ddot{U}_3 \bar{\rho}. \end{cases} \tag{A.4}$$

29

In terms of displacements (U_3, φ_α), the above equations are revised as:

$$\begin{cases} F^{\mathrm{R}}_{\alpha\beta} (\varphi_\beta + U_{3,\beta}) - D_{\alpha\beta\xi\eta}\varphi_{\eta,\xi\beta} = 0, & \text{(A.5a)} \\ F^{\mathrm{R}}_{\alpha\beta} (\varphi_{\beta,\alpha} + U_{3,\beta\alpha}) = \ddot{U}_3\bar{\rho}. & \text{(A.5b)} \end{cases}$$

The displacements $(U_3, \varphi_\alpha)(x_1, t)$, solution to the wave equations (A.5), have the general following form:

$$\begin{cases} U_3(x_1, t) = \Re\left(\hat{U}_3 e^{j(\omega t - kx_1)}\right), & \text{(A.6a)} \\ \varphi_\alpha(x_1, t) = \Re\left(\hat{\varphi}_\alpha e^{j(\omega t - kx_1)}\right), & \text{(A.6b)} \end{cases}$$

where $\hat{U}_3$ and $\hat{\varphi}_\alpha$ are constants. Plugging these functions into equations (A.5), it follows that:

$$\begin{cases} F^{\mathrm{R}}_{\alpha\beta}\left(\hat{\varphi}_\beta - jk\delta_{\beta 1}\hat{U}_3\right) + k^2 D_{\alpha 11\eta}\hat{\varphi}_\eta = 0, & \text{(A.7a)} \\ F^{\mathrm{R}}_{1\beta}\left(-jk\hat{\varphi}_\beta - k^2\delta_{\beta 1}\hat{U}_3\right) + \omega^2\hat{U}_3\bar{\rho} = 0. & \text{(A.7b)} \end{cases}$$

We denote by $[\delta^h]$ the vector of dimension 3 representing the generalized displacements:

$$[\delta^h]^T = \left[\hat{U}_3, \hat{\varphi}_1, \hat{\varphi}_2\right]. \tag{A.8}$$

Equations (A.7) can be rewritten as:

$$[\mathcal{B}] \cdot [\delta^h] = 0, \tag{A.9}$$

where $[\mathcal{B}]$ is a 3×3 matrix identified as:

$$[\mathcal{B}] = \begin{bmatrix} \omega^2\bar{\rho} - k^2 F^{\mathrm{R}}_{11} & -jk F^{\mathrm{R}}_{11} & -jk F^{\mathrm{R}}_{12} \\ -jk F^{\mathrm{R}}_{11} & F^{\mathrm{R}}_{11} + k^2 D_{1111} & F^{\mathrm{R}}_{12} + k^2 D_{1121} \\ -jk F^{\mathrm{R}}_{21} & F^{\mathrm{R}}_{21} + k^2 D_{2111} & F^{\mathrm{R}}_{22} + k^2 D_{2121} \end{bmatrix}. \tag{A.10}$$

The dispersion relation of flexural waves for homogeneous plates is deduced from solving:

$$\det[\mathcal{B}] = 0, \tag{A.11}$$

which yields

$$\omega^2 = \frac{k^6 F^{\mathrm{R}}_{11}\left(D_{1111}D_{2121} - D^2_{1121}\right) + k^4 D_{1111}\left(F^{\mathrm{R}}_{11}F^{\mathrm{R}}_{22} - (F^{\mathrm{R}}_{12})^2\right)}{\bar{\rho}\left((F^{\mathrm{R}}_{11} + k^2 D_{1111})(F^{\mathrm{R}}_{22} + k^2 D_{2121}) - (F^{\mathrm{R}}_{12} + k^2 D_{2111})^2\right)}. \tag{A.12}$$

30

The tensors $F_{\alpha\beta}^{\mathrm{R}}$ and $D_{\alpha\beta\gamma\delta}$, being positive definite respectively imply that:

$$F_{11}^{\mathrm{R}} > 0, \quad F_{11}^{\mathrm{R}} F_{22}^{\mathrm{R}} - (F_{12}^{\mathrm{R}})^2 > 0$$

and

$$D_{1111} > 0, \quad D_{1111} D_{2121} - D_{1121}^2 > 0.$$

Furthermore, the wavenumber k being real implies that the matrix $\begin{pmatrix} F_{11}^{\mathrm{R}} + k^2 D_{1111} & F_{12}^{\mathrm{R}} + k^2 D_{2111} \\ F_{12}^{\mathrm{R}} + k^2 D_{2111} & F_{22}^{\mathrm{R}} + k^2 D_{2121} \end{pmatrix}$ is positive definite. Therefore, its determinant is always positive. Namely,

$$\left(F_{11}^{\mathrm{R}} + k^2 D_{1111}\right)\left(F_{22}^{\mathrm{R}} + k^2 D_{2121}\right) - \left(F_{12}^{\mathrm{R}} + k^2 D_{2111}\right)^2 > 0.$$

As a consequence, equation (A.12) admits two real roots corresponding to the forward and backward flexural waves.

References

G. Kirchhoff, Über das gleichgewicht und die bewegung einer elastischen scheibe., Journal für die reine und angewandte Mathematik 40 (1850a) 51–88.

G. Kirchhoff, Ueber die schwingungen einer kreisförmigen elastischen scheibe, Annalen der Physik 157 (1850b) 258–264.

A. E. H. Love, I. the small free vibrations and deformation of a thin elastic shell, Proceedings of the Royal Society of London 43 (1888) 352–353.

E. Reissner, The effect of transverse shear deformation on the bending of elastic plates, J. Appl. Mech. Eng. ASME 12 (1945) A69–A77.

R. D. Mindlin, Influence of rotatory inertia and shear flexural motions of isotropic elastic plates, Journal of Applied Mechanics 18 (1951) 31 – 38.

P. Ciarlet, P. Destuynder, Justification of the two-dimensional linear plate model., Journal de mecanique 18 (1979) 315–344.

P. G. Ciarlet, Plates and junctions in elastic multi-structures : An asymptotic analysis (1990).

P. G. Ciarlet, Mathematical Elasticity - Volume II: Theory of Plates, Elsevier Science Bv, 1997.

P. C. Yang, C. H. Norris, Y. Stavsky, Elastic wave propagation in heterogeneous plates, International Journal of Solids and Structures 2 (1966) 665 – 684.

J. M. Whitney, N. J. Pagano, Shear deformation in heterogeneous anisotropic plates, Journal of Composite Materials 6 (1970) 30.

J. M. Whitney, Stress analysis of thick laminated composite and sandwich plates, Journal of Composite Materials 6 (1972) 426–440.

J. N. Reddy, On refined computational models of composite laminates, International Journal for Numerical Methods in Engineering 27 (1989) 361–382.

A. K. Noor, M. Malik, An assessment of five modeling approaches for thermo-mechanical stress analysis of laminated composite panels, Computational Mechanics 25 (2000) 43–58.

E. Carrera, Theories and finite elements for multilayered, anisotropic, composite plates and shells, Archives of Computational Methods in Engineering 9 (2002) 87–140.

A. Lebée, K. Sab, A bending-gradient model for thick plates. part i: Theory, International Journal of Solids and Structures 48 (2011) 2878–2888.

K. Sab, A. Lebée, Homogenization of Heterogeneous Thin and Thick Plates, 2015.

A. Lebée, K. Sab, On the generalization of reissner plate theory to laminated plates, part ii: Comparison with the bending-gradient theory, Journal of Elasticity 126 (2015).

N. Pagano, Exact solutions for composite laminates in cylindrical bending, Journal of Composite Materials 3 (1969) 398–411.

N. Pagano, Influence of shear coupling in cylindrical. bending of anisotropic laminates, Journal of Composite Materials 4 (1970) 330–343.

A. Lebée, K. Sab, Homogenization of thick periodic plates: Application of the bending-gradient plate theory to a folded core sandwich panel, International Journal of Solids and Structures 49 (2012a) 2778 – 2792. Proceedings of International Union of Theoretical and Applied Mechanics Symposium.

A. Lebée, K. Sab, Homogenization of cellular sandwich panels, Comptes Rendus Mécaniques 340 (2012b) 320–337.

A. Lebée, K. Sab, Homogenization of a space frame as a thick plate: Application of the bending-gradient theory to a beam lattice, Computers and Structures 127 (2013).

O. Perret, A. Lebée, C. Douthe, K. Sab, The bending-gradient theory for the linear buckling of thick plates: Application to cross laminated timber panels, International Journal of Solids and Structures 87 (2016) 139 – 152.

A. Lebée, K. Sab, Justification of the Bending-Gradient Theory Through Asymptotic Expansions, Springer Berlin Heidelberg, Berlin, Heidelberg, pp. 217–236.

N. Bejjani, K. Sab, J. Bodgi, A. Lebée, The bending-gradient theory for thick plates: Existence and uniqueness results, Journal of Elasticity 133 (2018) 37–72.

E. Kausel, Wave propagation in anisotropic layered media, International Journal for Numerical Methods in Engineering 23 (1986) 1567–1578.

S. K. Datta, A. H. Shah, R. L. Bratton, T. Chakraborty, Wave propagation in laminated composite plates,

The Journal of the Acoustical Society of America 83 (1988) 2020–2026.

H. Gravenkamp, C. Song, J. Prager, A numerical approach for the computation of dispersion relations for plate structures using the scaled boundary finite element method, Journal of Sound and Vibration 331 (2012) 2543 – 2557.

J. Renno, E. Manconi, B. Mace, A finite element method for modelling waves in laminated structures, Advances in Structural Engineering 16 (2013) 61–76.

P. Margerit, Caractérisation large bande du comportement dynamique linéaire des structures hétérogènes viscoélastiques anisotropes. Application à la table d'harmonie du piano, Ph.D. thesis, Université Paris-Est, 2018.

A. Lebée, K. Sab, A bending-gradient model for thick plates, part ii: Closed-form solutions for cylindrical bending of laminates, International Journal of Solids and Structures 48 (2011) 2889–2901.

A. Lebée, K. Sab, On the generalization of reissner plate theory to laminated plates, part i: Theory, Journal of Elasticity 126 (2015).

H. Lamb, On waves in an elastic plate, Proceedings of the Royal Society of London. Series A, Containing Papers of a Mathematical and Physical Character 93 (1917) 114–128.

W. T. Thomson, Transmission of elastic waves through a stratified solid medium, Journal of Applied Physics 21 (1950) 89 – 93.

N. Haskell, The Dispersion of Surface Waves on Multilayered Media, American Geophysical Union (AGU), pp. 86–103.

H. Schmidt, G. Tango, Efficient global matrix approach to the computation of synthetic seismograms, Geophysical Journal of the Royal Astronomical Society 84 (2007) 331 – 359.

A. H. Nayfeh, The general problem of elastic wave propagation in multilayered anisotropic media, The Journal of the Acoustical Society of America 89 (1991) 1521–1531.

S. Rokhlin, L. Wang, Stable recursive algorithm for elastic wave propagation in layered anisotropic media: Stiffness matrix method, The Journal of the Acoustical Society of America 112 (2002) 822–34.

S. Dong, R. B. Nelson, On natural vibrations and waves in laminated orthotropic plates, Journal of Applied Mechanics 39 (1972).

Z. C. Xi, G. R. Liu, K. Y. Lam, H. M. Shang, Dispersion and characteristic surfaces of waves in laminated composite circular cylindrical shells, The Journal of the Acoustical Society of America 108 (2000) 2179–2186.

P. J. Shorter, Wave propagation and damping in linear viscoelastic laminates, Journal of The Acoustical Society of America - J ACOUST SOC AMER 115 (2004).

E. Barbieri, A. Cammarano, S. D. Rosa, F. Franco, Waveguides of a composite plate by using the spectral finite element approach, Journal of Vibration and Control 15 (2009) 347–367.

33

I. Bartoli, A. Marzani, F. L. di Scalea, E. Viola, Modeling wave propagation in damped waveguides of arbitrary cross-section, Journal of Sound and Vibration 295 (2006) 685 – 707.

N. Bejjani, The Bending-Gradient flexural dispersion curves, 2019. Https://github.com/Nadinebejjani/Bending-Gradient.git.

Z. Liu, M. Fard, J. Davy, Prediction of the effect of porous sound-absorbing material inside a coupled plate cavity system, International Journal of Vehicle Noise and Vibration 12 (2016) 314.